NIST Measurement Services:

Calibration Service for Spectral Responsivity of Laser and Optical-Fiber Power Meters at Wavelengths Between 0.4 μm and 1.8 μm

NIST
Special
Publication
250–53

John H. Lehman

U.S. Department of Commerce
Technology Administration
National Institute of Standards and Technology

National Institute of Standards and Technology Special Publication 250–53
Natl. Inst. Stand. Technol. Spec. Publ. 250–53, 41 pages (Dec. 1999)
CODEN: NSPUE2

U.S. GOVERNMENT PRINTING OFFICE
WASHINGTON: 1999

For sale by the Superintendent of Documents, U.S. Government Printing Office, Washington, DC 20402–9325

Contents

Calibration Service for Spectral Responsivity of Laser and Optical-Fiber Power Meters at Wavelengths between 0.4 μm and 1.8 μm

John H. Lehman
National Institute of Standards and Technology
Optoelectronics Division
325 Broadway
Boulder, Colorado 80303

This document describes a calibration service for absolute spectral-responsivity measurements of laser power meters, optical-fiber power meters, and detectors used with lasers and optical-fiber connectors at wavelengths between 400 nm and 1800 nm. In addition to a summary of the calibration procedure, a theoretical basis is given for the uncertainty assessment, as well as an overview of the measurement system and operating procedures. A sample calibration report is included in this document that is similar to that which is provided to the customer. The calibration report contains absolute responsivity in terms of amps per watt at each wavelength increment and a summary of the uncertainty assessment for the meter.

Keywords:
absolute spectral responsivity; laser power; optical-fiber power; optical detector calibration; optical fiber connector; photodetectors; pyroelectric detectors

1. Introduction

This calibration service provides absolute spectral-responsivity measurements of laser power meters, optical-fiber power meters, and detectors used with lasers and optical-fiber connectors at wavelengths between and beyond those available from other NIST laser calibration services. The measurements are made at 10 nm increments over wavelengths from 400 nm to 1800 nm using a monochromator-based system, and are normalized to higher accuracy measurements made with laser sources in this range (see NIST calibration services 42130C – 42131C and 42110C – 42111C) [1,2]. In each calibration, particular care is taken to evaluate the effects of source coherence, interference, and reflections on the quality of the calibration; these factors generally dominate estimates of uncertainty.

The appropriate calibration procedure and the calibration uncertainty must be interpreted case-by-case, depending on the intended use and nature of the test meter [3,4]. This determination begins prior to the measurement, with a dialogue with the customer to understand the meter's intended use and physical configuration. For each meter (or detector module) sent to NIST for calibration, the customer is provided a written calibration report. The calibration report contains absolute responsivity in terms of amps per watt at each wavelength increment, a brief description of the measurement system and procedure, and a summary of the uncertainty assessment. Information unique to the individual calibration will

also be included.

For silicon photodiode-based meters, the wavelength range for the service is normally 450 nm to 1000 nm, and for meters that incorporate photodiodes made from germanium or indium gallium arsenide, the range is 800 nm to 1750 nm. If necessary, this coverage may be shortened or slightly extended. We have an ongoing effort to include into the measurement procedure comparisons with a greater number of laser sources that are not listed as part of 42130C and 42131C (currently 670 nm, 780 nm, 850 nm, 980 nm, 1310 nm, and 1550 nm). Such comparisons provide information that may reduce the measurement uncertainty. The customer is invited to inquire about the use of other laser wavelengths for which calibration may be provided as a special test.

2. 42164C Calibration Service Summary

When we calibrate an optical-fiber power meter for absolute spectral responsivity, we acquire one data set from a monochromator-based measurement system and two additional independent data sets from a laser-based measurement system, with and without fiber connectors installed [5]. Our first data set is a measure of the meter's absolute spectral responsivity over the entire wavelength range of the meter. These data are usually depicted as a smooth curve consisting of absolute responsivity values at 10 nm increments. The second set represents the meter's absolute responsivity at several discrete laser wavelengths, for example 850 nm, 1310 nm, and 1550 nm. The third set is similar to the second, except that the laser light is coupled to the meter and the transfer-standard detector using a fiber optic cable and connector. Differences in the three data sets reveal possible offsets that may result from the use of a particular fiber connector.

The detector input conditions for this procedure include at least two of the following scenarios as shown in Fig. 1. In scenario A of Fig. 1, collimated, coherent light is directed at the detector surface. In scenario B, light from either a coherent or incoherent source is focused at or near the detector surface. In scenario C, light is transmitted through a fiber attached to the detector with a fiber connector. Typically, light from a single-mode fiber has a divergence angle that is less than 14° (±7° from normal incidence). In most cases, the fiber connector functions as an enclosure. Light from the fiber is reflected between the detector and the fiber connector, and the reflectance of the fiber connector varies as a function of wavelength. In the context of our calibration service, an ideal laser power meter would have the same absolute spectral responsivity for each of these three scenarios [6]. (Note: Thermal detectors with a black absorbing surface, such as our pyroelectric-based reference detector, often meet these conditions, but generally require the use of a chopper and are therefore not suitable for fiber systems [7].)

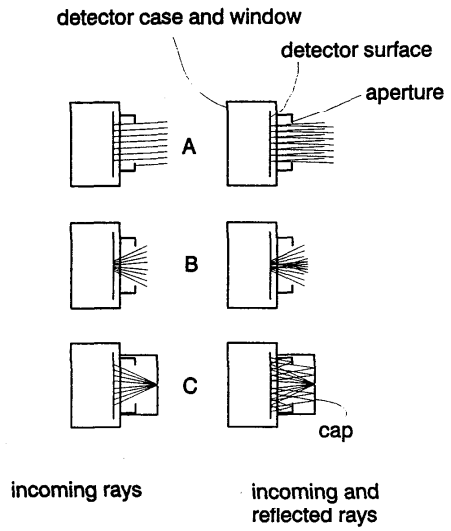

Figure 1. Optical input conditions: a. collimated; b. converging; c. diverging from fiber connector.

The correct results and the preferred calibration procedure depend on the intended use of the customer's meter. Figure 2 shows an example of an absolute responsivity curve obtained using the monochromator-based measurement system. Also shown as solid circles are the connectorized, laser-based measurement system results for the same detector. If the laser or optical-fiber power meter is intended to be used with fiber connectors attached, we shift the entire curve obtained using the monochromator-based system (without changing its shape), so that it agrees as closely as possible with the results obtained using the laser-based measurement system. The amount of shift and the resulting uncertainty are calculated based on the difference between the laser-based measurement results and the monochromator-based measurement results. In this example, the customer would be provided with absolute-responsivity values corresponding to 10 nm wavelength increments, from 750 nm to 1800 nm (the data from which the curve is drawn). One uncertainty value would be given for the entire curve.

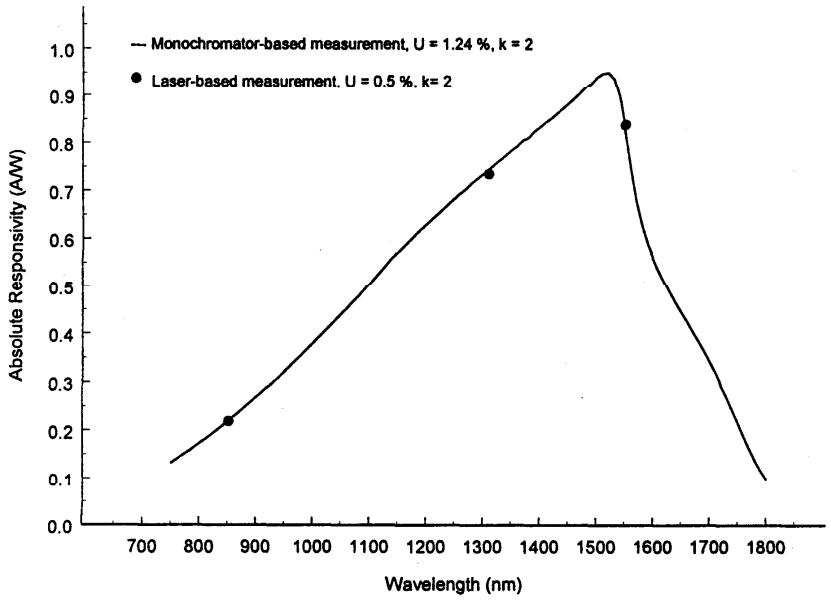

Figure 2. Absolute spectral responsivity results. The line is obtained from the monochromator-based measurement system (each datum spaced at 10 nm increments). The solid circles are results from the fiber-connector, laser-based measurement system.

3. Design Philosophy and Theory

A conventional technique for developing the measurement equation for an optical radiation measurement is given in detail by Kostkowski and Nicodemus [8]. In this section we briefly describe the measurement configuration (details are given in section 4) and present a measurement equation along with assumptions that allow us to define a closed solution. Using this foundation, we describe the measurement uncertainties in section 6, in a way that will hopefully be beneficial to the calibration customer.

The definition of spectral responsivity for an optical detector is based on the observation that the electrical output (photocurrent) of a detector is proportional to the optical input (flux, radiant flux, or radiance). The mathematical relationship for the electrical output $X(\lambda)$, of an optical detector is the following:

$$X(\lambda) = \Phi(\lambda) \cdot S(\lambda), \tag{1}$$

where $\Phi(\lambda)$ is the flux and $S(\lambda)$ is the detector responsivity. This measurement equation assumes that the detector responsivity $S(\lambda)$ is spatially uniform, and that the detector is

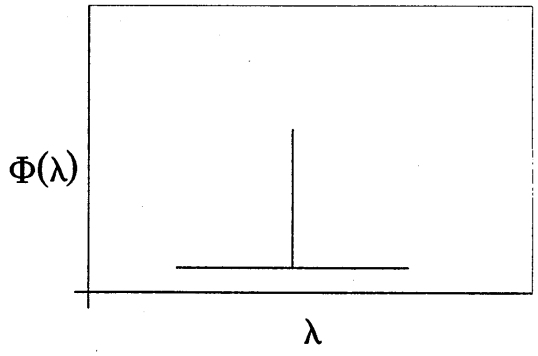

Figure 3. Ideal source.

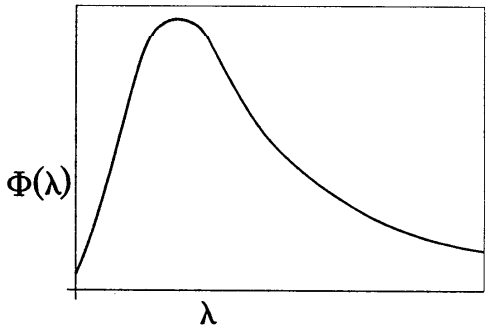

Figure 4. Broadband lamp output.

uniformly irradiated by an ideal optical source. The ideal source has flux $\Phi(\lambda)$, is unpolarized, and has infinitely narrow bandwidth at wavelength λ (this is depicted in Fig. 3).

The monochromator-based system does not satisfy the criterion for Fig. 3, so we must modify the measurement equation so that it is appropriate for our monochromator-based system. Using functions based on properties of the light source, monochromator, and other optical elements, we progress toward a much more complicated expression for approximately the same spectrum *shape* introduced in Fig. 3. We begin with a broadband source having a spectrum that is approximately the shape of an ideal blackbody, shown in Fig. 4.

The monochromator throughput, shown in Fig. 5, varies as a function of wavelength depending on the grating efficiency. We include an efficiency term, $E^0(\lambda)$ in the measurement equation to account for this variability. The details are not shown in the figure, but the radiance and polarization of light from the monochromator vary as a function of wavelength. We later account for these affects by including the detector's linearity and polarization sensitivity in our uncertainty assessment.

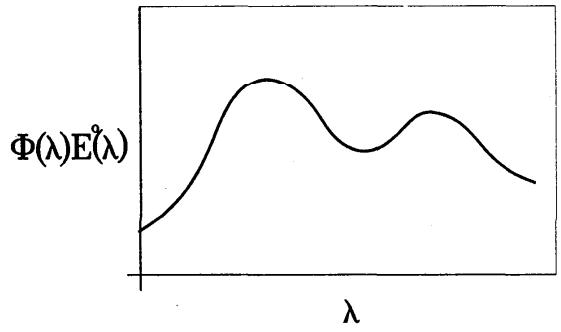

Figure 5. Lamp output, monochromator efficiency, $\Phi(\lambda)\ E^0(\lambda)$.

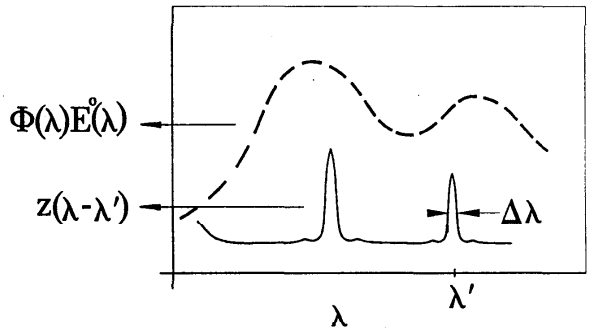

Figure 6. Lamp output, monochromator efficiency, and slit scattering; $\Phi(\lambda)E^0(\lambda)$, $z(\lambda - \lambda')$.

Rotation of the grating relative to the monochromator slits determines the wavelength that will pass a defined band, $\Delta\lambda$, through the exit slit. In addition, two other phenomena may be seen at the exit slit of the monochromator: (1) light that is predictable and unwanted, for example, multiple orders of a given wavelength (coherent scattering); and (2) background light such as incoherent scattering from the grating and other optical elements. We partially account for this added complexity with a slit scattering function, $z(\lambda - \lambda')$. The superposition of the slit scattering on the lamp and grating efficiency is shown in Fig. 6. (note: The term slit scattering is often used for this function, but it is not really descriptive and a bit confusing. The term refers to scattering from the grating, both coherent and incoherent, that appears at the exit slit of the monochromator (not scattering by the slits)).

Most of the coherent scattered light, depicted in Fig. 6, is eliminated using a longpass filter as shown in Fig. 7. The filter transmittance function, along with the transmittance function of other optical elements in the system such as mirrors outside the monochromator, appears in the measurement equation as $T(\lambda)$.

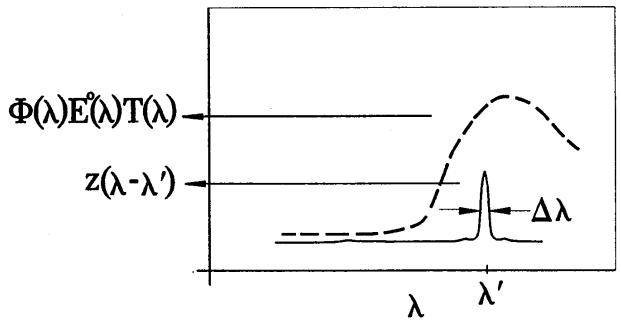

Figure 7. Lamp output, monochromator efficiency, filter and mirror transmittance, and slit scattering; $\Phi(\lambda)E^0(\lambda)T(\lambda)$, $z(\lambda - \lambda')$.

We use the terms introduced above and include another term X_{sl} in the measurement equation which accounts for all scattered light, so that the measurement equation is now:

$$X(\lambda) = \Phi(\lambda) \cdot S(\lambda) \cdot T(\lambda) \cdot E(\lambda) + X_{sl}(\lambda). \quad (2)$$

X_{sl} represents an average of the out-of-band light in the path of the lamp output (the preferred source light). Accordingly, we expand X_{sl} in the equation above to:

$$X_{sl}(\lambda) = \int_{\lambda <> \Delta\lambda} \Phi(\lambda') \cdot S(\lambda') \cdot T(\lambda') \cdot E(\lambda') \cdot d\lambda'. \quad (3)$$

Note that the notation λ' is switched with λ to be consistent with eq (1). Also, beginning with eq 2, Φ, E^0, and T are constant over $\Delta\lambda$.

Now the measurement equation is:

$$X(\lambda) = \Phi(\lambda) \cdot S(\lambda) \cdot T(\lambda) \cdot E(\lambda) + \int_{\lambda <> \Delta\lambda} \Phi(\lambda') \cdot S(\lambda') \cdot T(\lambda') \cdot E(\lambda') \cdot d\lambda', \quad (4)$$

where

$$E(\lambda) = E^0(\lambda) \int_{\Delta\lambda} z(\lambda - \lambda') \cdot d\lambda', \text{ and } E(\lambda') = E^0(\lambda') \int_{\lambda <> \Delta\lambda} z(\lambda - \lambda'') \cdot d\lambda'. \quad (5)$$

In real monochromators, there is some residual spectral component to $z(\lambda - \lambda')$ outside the bandpass due to scattered light, zero order leakage, and grating ghosts, but this component is difficult to fully evaluate and correct. (We estimate the uncertainty for the monochromator efficiency and scattered light in section 6.2.1.2.) For more information, the efficiency and slit scattering functions are discussed by Kostkowski and Nicodemus [8]. Because our measurement configuration uses a single monochromator with longpass filters and has relatively high scattered light compared to double monochromator systems, we carry this residual through the final measurement equation.

To proceed, we revert to a form similar to our original equation, but, with an

understanding of what is included, we write a simplified measurement equation that is not only suitable for monochromator-based spectral responsivity but also for the substitution (or comparison) method. In the following discussion, subscript ***t*** designates the test detector, subscript ***s*** designates the standard reference detector, and the additional *sl* is carried throughout to designate the scattered-light residual as the integral in eq (5). In addition, the λ-function notation is dropped for simplicity.

For detector electrical output X, responsivity S, and optical input M (at the detector), we can write

$$X_t = M_t \cdot S_t + X_{tsl} \qquad \text{and} \qquad M_s = \frac{(X_s - X_{ssl})}{S_s}. \tag{6}$$

In our measurement configuration, the reference detector is the basis for M and because of the short measurement duration at each wavelength of interest and the stability of the lamp source, we assume (with some uncertainty given in section 6.1.2) that $M_t = M_s$. Therefore

$$S_t = \frac{(X_t - X_{tsl})}{(X_s - X_{ssl})} \cdot S_s. \tag{7}$$

In practice, offsets in the detectors and instrumentation require the measurement of signals without optical inputs to determine baseline levels, in effect, non-optical background. This is included where necessary and may be stated as

$$S_t = \frac{(X_t - X_{tsl} - X_t^{offset})}{(X_s - X_{ssl} - X_s^{offset})} \cdot S_s. \tag{8}$$

It is also common to include the gain G, of any electronic amplifiers used with the test and reference detectors. For our measurement configuration, this leaves a final measurement equation of

$$S_t = \frac{(X_t - X_{tsl} - X_t^{offset})}{(X_s - X_{ssl} - X_s^{offset})} \cdot \frac{G_s}{G_t} \cdot S_s. \tag{9}$$

4. Measurement System

The spectral responsivity of the customer's meter is measured using the system shown schematically in Fig. 8. The essential components include a tungsten filament lamp source and a single-grating monochromator (Czerny-Turner configuration) with order-sorting colored-glass filters. The light path is extended using mirrors on both the input and output of the monochromator, to accommodate a variety of shapes and sizes of meters. A translation stage on the input side of the monochromator allows a chopper to be moved in and out of the beam path, to accommodate the reference detector. A flat mirror on a rotary stage on the output side of the monochromator allows light to alternate between the reference detector and the test detector.

Normally, the beam is focused (F number ≅ f/4) to a radius of approximately 2 mm

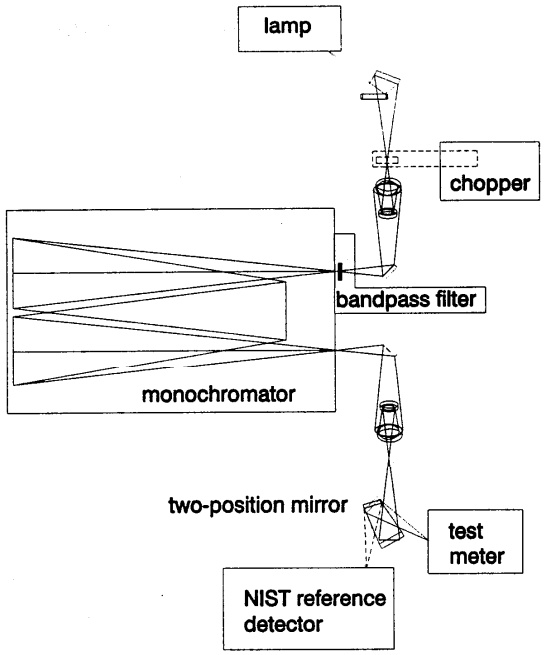

Figure 8. Grating monochromator-based spectral responsivity measurement system.

at the position of, and normal to, the plane of the test meter. The bandpass of the monochromator is less than 6 nm.

A pyroelectric detector is used as the reference detector for all measurements. The reference detector is actively thermally stabilized and is electrically connected to dedicated current amplifier, lock-in amplifier, and optical chopper.

Optics and instrumentation used with the monochromator output are enclosed in a light-tight box. The entire measurement system rests on a commercial, vibration-damping tabletop. All instruments, including the customer's meter and the monochromator, are controlled using GPIB/IEEE hardware connections.

4.1 Hardware

4.1.1 Light Source

The broad-spectrum light source is a tungsten-filament, quartz-envelope light bulb. The dimensions of the filament are specified by the manufacturer as 4.1 mm × 9.5 mm. The bulb has a rated filament temperature of 3400 K, at 6.25 A and 24 V. The light source is controlled using a dedicated electrical power supply operating in a constant-current mode. The drift of the lamp power output has been measured to vary less than 0.1 % over a 30 minute period.

4.1.2 Monochromator

4.1.2.1 Gratings

The monochromator grating is mounted in a Czerny-Turner configuration. One of

two gratings is available, depending on the wavelength range of the desired calibration. The ruling density of each grating is 600 lines/mm. One grating is blazed at 500 nm and the other at 1000 nm. The useful range of the monochromator using both gratings is 400 nm to 1800 nm. The grating is moved using a stepper motor coupled to an absolute encoder. The stepper motor is coupled to a lead screw that drives a sine-bar mechanism. The grating is attached to a kinematic mount, and, because each grating has the same line density, the grating position algorithm is calibrated using a single offset value. The stepper motor is capable of up to 50,000 steps per revolution. The encoder will resolve 16384 steps per revolution. With the use of a grating ruled with 600 grooves per millimeter, the mechanical relationship of the grating placement and the wavelength selection is 10 nm per revolution. Therefore, the mechanism is capable of 1638.4 steps per nm. This implies a positioning resolution of 0.0006 nm. However, the grating resolution is the practical limit. According to the grating equation, the resolution is theoretically 0.06 nm [9,10]. Realistically, the measurement resolution is decreased by the need for increased throughput. To increase the throughput, the monochromator input and output aperture slits are widened to about 2 mm and limit the resolution to about 6 nm for measurement test conditions.

4.1.2.2 Glass Filters (Bandpass Filters)

Colored glass filters are used to reduce transmission of the unwanted orders reflected by the gratings and to reject stray light. The gratings are chosen to maximize throughput and also to minimize the magnitude of overlapping orders over the useful wavelength range. Four filters are used [11]. The wavelength range of each filter is as follows:

450 nm – 670 nm: OptoSigma 079-3340
670 nm – 1075 nm: Schott LL 0650
1075 nm – 1575 nm: Schott LL 1000
1575 nm – 1800 nm: Schott RL 1500

The filters are mounted on a motorized disk that rotates each filter into the path of the input light, for each wavelength range.

4.1.3 Optical System

Several mirrors are used outside of the monochromator to collect light from the lamp and focus light onto each detector. The mirror surfaces are silver with a dielectric overcoat and are located at nearly symmetrical positions at the monochromator input and output. Two spherical mirrors with an f-number of f/2 are used to collect light and extend the working distance from the source and detectors using a 1:1 image distance. The mirror configuration is shown in Fig. 9.

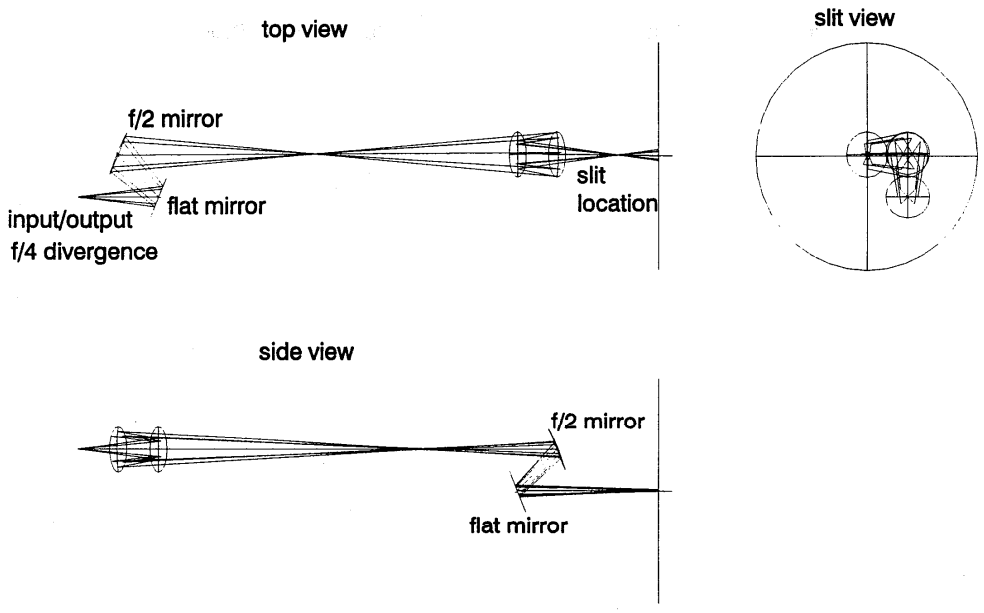

Figure 9. Geometrical ray tracing of input optics outside the monochromator in three orthogonal views (output optics are identical).

When light is reflected from the first spherical mirror and is directed off-axis, aberration is introduced. To achieve the theoretical resolution of the grating, this aberration must be minimized. The second spherical mirror directs the light in an orthogonal plane to partially correct the aberration.

There are two more mirrors inside the monochromator. These mirrors are f/4.7 and are approximately 150 mm × 150 mm square. One mirror collimates light from the input slit and directs it to the grating, while the other focuses light on the exit slit of the monochromator. These two mirrors are front-surface aluminum mirrors with a magnesuim fluoride overcoat.

4.1.4 Enclosure

The monochromator grating, monochromator mirrors, bandpass filters, test and reference detectors, and output optics and fixtures of the monochromator are enclosed in a light-tight box. The only normally detectable light (more than a picowatt) transmitted to the test and reference detector enters the measurement system through the slit on the lamp side of the monochromator. The lamp, data acquisition system, and chopper are the only significant components that are not enclosed.

4.1.5 Data-Acquisition System

The electronic hardware is controlled using a personal computer based on an Intel 80486/120MHz processor and a GPIB card. Communications protocol is based on the IEEE/GPIB interface standard.

4.2 Software

The software is written to control the electronic instrumentation and collect data over the GPIB. The interface is written to resemble a virtual instrument with push buttons, slider keys, and numerical and graphical displays. By use of the software one can set the positioning stage locations, adjust the lamp current and voltage, control the detector electronics, and set up data collection parameters. During a data-collection episode, the wavelength scan range, time delays, file destinations, and number of data points to average can be input into the program.

4.3 Reference Detector (Transfer Standard)

4.3.1 Pyroelectric Wedge Trap Detector (PWTD) Design Attributes

The reference detector is a pyroelectric trap built and evaluated at NIST. The trap design is based on a lithium tantalate ($LiTaO_3$), pyroelectric disc coated with gold black, positioned opposite a gold mirror in a wedge configuration. The low-reflectance gold black coating, along with the wedge-trap structure, ensure that the pyroelectric disc absorbs 99 % of the light entering the aperture [7]. A schematic figure of the reference detector design is shown in Fig. 10. The multiple-reflection wedge-shaped trap structure has a 5 mm diameter input aperture and an f/4 field of view.

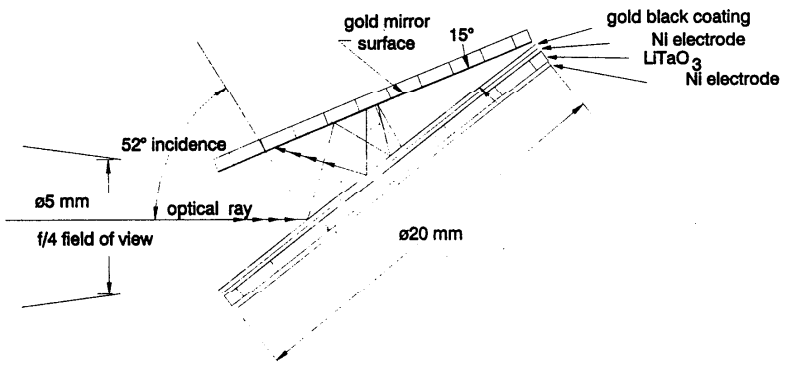

Figure 10. Cross-section view of the pyroelectric wedge-trap detector. Light rays entering the trap cavity, within the f/4 field of view have at least four chances to be absorbed by detector element (for specularly reflected rays).

4.3.2 Performance

Pyroelectric detectors that are designed for radiometric applications typically demonstrate spatial uniformity variations of ± 2 %, noise equivalent power (NEP) ranging from 10^{-7} W/Hz$^{1/2}$ (no window) to less than 10^{-8} W/Hz$^{1/2}$ (small area, sealed container with a window), and a wavelength sensitivity ranging from the visible to beyond 10 μm. Despite years of development and commercial success, these numbers do not represent the theoretical performance limits for pyroelectric detectors. Although we have not yet reached the theoretical limits of performance, we have achieved a design compromise that optimizes those detector properties that are important for high accuracy spectral responsivity and absolute power measurements. The transfer standard for this measurement system has a responsivity that varies as a function of wavelength by less than 1% over a range from 0.4 μm to 1.8 μm and has a measured NEP of 5x10^{-8} W/Hz$^{1/2}$.

Knowledge of the spatial uniformity of a detector is particularly important for measurements that require varying beam-input conditions (such as diverging versus collimated input beams or repeated detector alignment). We measured the spatial uniformity over the PWTD aperture area using a 0.3 mm diameter, circularly polarized, 674 nm laser beam as a probe. This probe beam was scanned across the aperture area at 0.1 mm intervals while detector output data were collected. The data, plotted in Fig. 11, show that the maximum variation in detector response is less than 1% over an area roughly 5 mm in diameter.

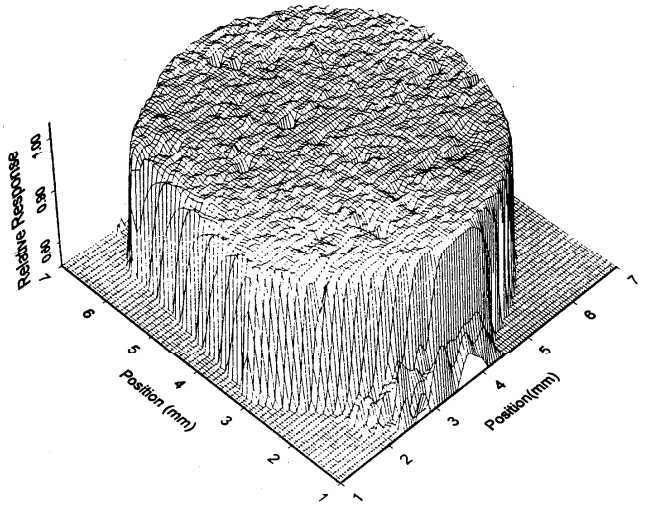

Figure 11. Spatial uniformity of PWTD.

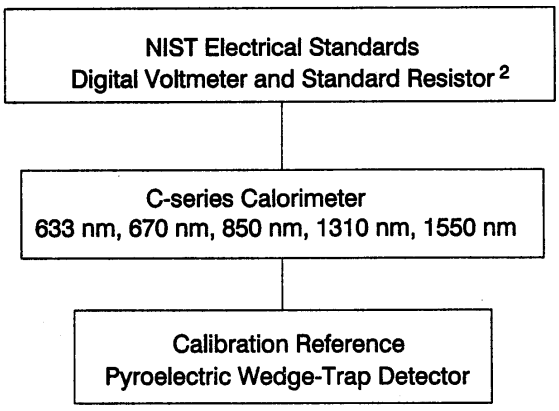

Figure 12. Pyroelectric wedge-trap detector traceability.

4.3.3 Calibration and Traceability

In principle, the pyroelectric wedge trap (PWTD) responsivity is constant (uniform) over the entire spectrum of interest for this calibration service. We verify this assumption by comparing the relative responsivity of the PWTD to several transfer-standard detectors that are traceable to NIST. In addition, the relative spectral responsivity of the reference detector has been measured using a large-area pyroelectric detector, which incorporates a gold-plated integrating hemisphere [12]. The primary traceability of the PWTD is absolute responsivity measured using laser input sources at 633 nm, 670 nm, 850 nm, 1310 nm, and 1550 nm compared to the NIST C-series calorimeter (see Fig. 12 below), which is traceable to NIST electrical standards [2].

5 Operating Procedures

5.1 Wavelength Verification

The monochromator uses two different gratings. Though the kinematic mounts built into each grating are quite reliable, it is recommended that the calibration be checked after each grating change. Several helium neon laser lines are used to check the wavelength calibration at approximately 633 nm, 1165 nm, 1176 nm, and 1523 nm. The monochromator is scanned over a region near these wavelengths, with a slit width of 0.5 mm, to determine whether the monochromator shows an offset from expected peaks. If necessary, an offset is added to the control software that turns the grating stepper motor. Two gratings cover the wavelength range of the calibration service, to minimize the dependence of grating efficiency with increasing wavelength.

5.2 Startup

Before any measurement is performed, the system is allowed to warm up at full

power. In this case, full power means the lamp source is at 150 W, all electronics are turned on, the positioning stages are initialized, and the reference-detector thermoelectric cooler is on and is allowed to achieve the desired temperature setpoint. The control program is initialized and all instruments in the measurement system may be tested to insure the GPIB is operating properly.

5.3 Monochromator Alignment

After the system has warmed up for about an hour, slight adjustments may be made to the first mirror, which collects light from the lamp source. Adjusting this mirror will optimize the amount of power incident at the entrance slit of the monochromator and, ultimately, the amount of power incident on both detectors. For wavelength-calibration purposes, the first mirror may also be rotated several degrees, to collect light from a laser or gas-lamp source.

5.4 Detector Alignment and Measurement Protocol

The calibration-measurement process begins by adjusting the monochromator so that it transmits a visible filament image. This image is centered onto the reference detector. The two-position mirror is then moved to the complementary position, and the test meter is aligned as necessary. The test detector must capture all the incident light to insure that an absolute measurement is accurate. The detector must also be aligned so that the incident light is perpendicular to the detector. Both detectors are enclosed in the light-tight box. Next, the GPIB communication is established with the test meter, and appropriate settings are made, including any offsets. Using the *scan parameters* menu, *starting wavelength, ending wavelength, wavelength increment, test meter pause for data,* and the number of data points to average is selected. *Begin wavelength scan* may now be selected and the data will be acquired as follows:

1. Adjust monochromator grating and filters to *starting wavelength.*
2. Send chopper to home position for reference detector.
3. Send two-position mirror to home position for reference detector.
4. Pause and then acquire and store data from the reference detector ($n_s = 40$).
5. Send chopper out of the light path.
6. Send two-position mirror to test position for test detector.
7. Pause and then acquire and store data from test detector ($n_t = 5$).
8. Repeat steps 2 through 7, two more times.
9. Adjust monochromator by the *wavelength increment.*
10. Repeat steps 2 through 8 until the *ending wavelength.*

5.5 Data Acquisition

The sequence and duration of the data acquisition represents a compromise that is an attempt to maximize data-averaging in a minimum amount of time. The random uncertainty associated with the pyroelectric reference detector increases with decreasing monochromator throughput. The random uncertainty will decrease as more data are acquired. However, to reduce the random uncertainty by an order of magnitude requires several minutes of additional data at each wavelength increment (using a reference-detector time constant of one second and acquiring forty samples per data point). Typically, acquiring

a complete set of spectral responsivity data for a semiconductor-based power meter will take several hours.

For each wavelength interval, the data acquisition sequence is as follows. Light from the monochromator is first directed at the reference detector. The acquisition program pauses approximately 40 s, until the reference detector achieves a nearly steady- state value. Then, 40 data samples are taken, spaced 1 s apart, and the average value is recorded. Next, light is directed at the test detector for a duration and sample time prescribed by the manufacturer or customer; this data sample set is averaged and recorded. This process is repeated two more times for each wavelength. Ideally, the pause duration and sample-set size for each detector and for each wavelength are based on achieving a normal distribution over some interval, centered over the sample-set average. Realistically, the distribution is an approximation of the normal distribution, because practical time constraints limit the number of data points that can be taken.

The format for the data acquisition is shown in table 1. Following this, in eq (10), is the formulation for calculating the responsivity of the test detector at a given wavelength. The customer is provided a table with a calibration report (see Appendix B), indicating the responsivity $S_t(\lambda)$ for each λ over the wavelength range.

Table 1. Data for calculation of responsivity for each wavelength increment.

Wavelength (sampling repeated 3 times at each wavelength)	NIST reference data	NIST reference background*	Test data	Test background*
S(1) (λ_1 = starting wavelength)	$X(1)_{s1}$, $X(1)_{s2}$, $X(1)_{s13}$,...$X(1)_{s40}$	$b(1)_{s1}$, $b(1)_{s2}$, $b(1)_{s3}$,...$b(1)_{s40}$	$X(1)_{t1}$, $X(1)_{t2}$, $X(1)_{t3}$, ...$X(1)_{t5}$	$b(1)_{t1}$, $b(1)_{t2}$, $b(1)_{t3}$, ...$b(1)_{t5}$
S(2) (λ_1 + increment)	$X(2)_{s1}$, $X(2)_{s2}$, $X(2)_{s3}$,...$X(2)_{s40}$	$b(2)_{s1}$, $b(2)_{s2}$, $b(2)_{s3}$, ...$b(2)_{s240}$	$X(2)_{t1}$, $X(2)_{t2}$, $X(2)_{t3}$, ...$X(2)_{t5}$	$b(2)_{t1}$, $b(2)_{t2}$, $b(2)_{t3}$, ...$b(2)_{t5}$
S(3) (λ_2 + increment)	$X(3)_{s1}$, $X(3)_{s2}$, $X(3)_{s3}$,...$X(3)_{s40}$	$b(3)_{s1}$, $b(3)_{s2}$, $b(3)_{s3}$, ...$b(3)_{s340}$	$X(3)_{t1}$, $X(3)_{t2}$, $X(3)_{t3}$, ...X_{t5}	$b(3)_{t1}$, $b(3)_{t2}$, $b(3)_{t3}$, ...$b(3)_{t5}$
S(j) (λ_{j-1} + increment)...	...	...	...	...
S(f) (ending wavelength)	$X(f)_{s1}$, $X(f)_{s2}$, $X(f)_{s3}$, ...$X(f)_{s40}$	$b(f)_{s1}$, $b(f)_{s2}$, $b(f)_{s3}$, ...$b(f)_{s40}$	$X(f)_{t1}$, $X(f)_{t2}$, $X(f)_{t3}$, ...$X(f)_{t5}$	$b(f)_{t1}$, $b(f)_{t2}$, $b(f)_{t3}$, ...$b(f)_{t5}$

* combined $b = X_{si} + X^{offset}$ as appropriate

$$S(j)_t = 1/3\left[\left(\frac{\frac{\sum_{i=1}^{5} X_{ti}}{5} - \frac{\sum_{i=1}^{5} b_{ti}}{5}}{\frac{\sum_{i=1}^{40} X_{si}}{40} - \frac{\sum_{i=1}^{40} b_{si}}{40}}\right)_{\lambda=j} + \left(\frac{\frac{\sum_{i=1}^{5} X_{ti}}{5} - \frac{\sum_{i=1}^{5} b_{ti}}{5}}{\frac{\sum_{i=1}^{40} X_{si}}{40} - \frac{\sum_{i=1}^{40} b_{si}}{40}}\right)_{\lambda=j}^{\substack{\text{reposition} \\ \text{repeat}}} + \left(\frac{\frac{\sum_{i=1}^{5} X_{ti}}{5} - \frac{\sum_{i=1}^{5} b_{ti}}{5}}{\frac{\sum_{i=1}^{40} X_{si}}{40} - \frac{\sum_{i=1}^{40} b_{si}}{40}}\right)_{\lambda=j}^{\substack{\text{reposition} \\ \text{repeat}}}\right] \cdot \frac{G_s}{G_t} \cdot S_s \quad \textbf{(10)}$$

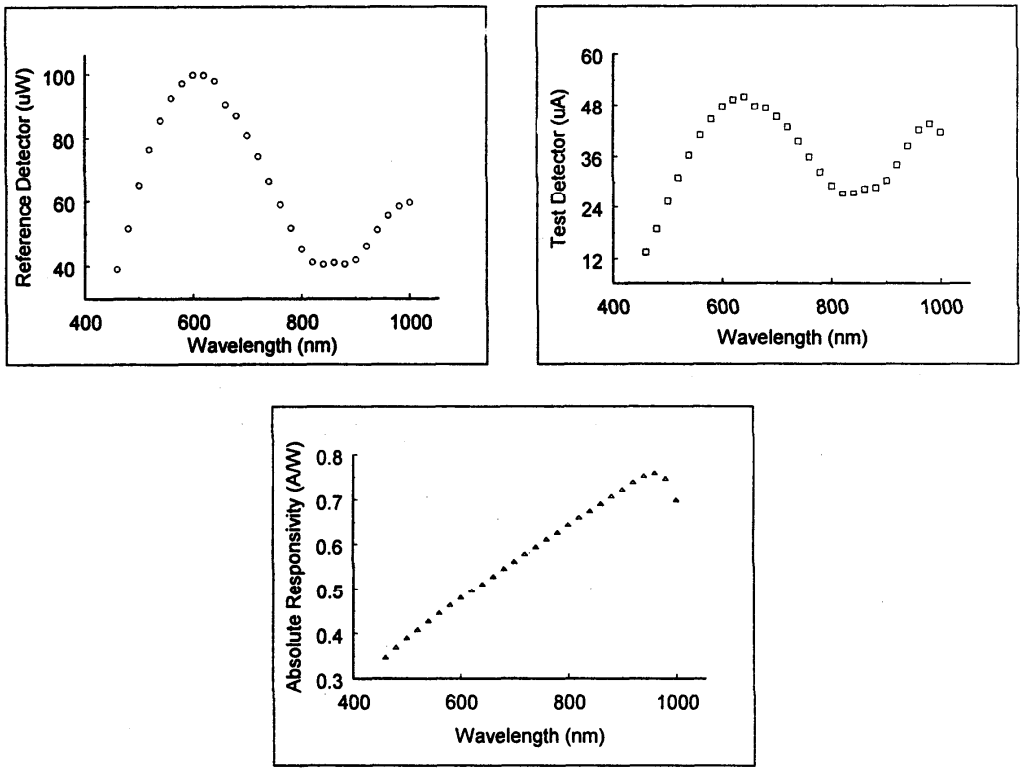

Figure 13. Spectral responsivity measurement results for a silicon photodiode-based optical detector.

Three graphs are shown in Fig. 13, which represent the averaged data for a sample measurement for the reference detector and for the test detector, as well as the calculated absolute responsivity of the test detector.

6. Uncertainty Assessment

The uncertainty estimates for the NIST spectral responsivity measurements are assessed using guidelines from NIST Technical Note 1297, "Guidelines for Evaluating and

Expressing the Uncertainty of NIST Measurement Results" by Barry N. Taylor and Chris E. Kuyatt, 1994 Edition [13]. To establish the uncertainty limits, the error sources are separated into (1) Type B errors, for which magnitudes are determined by subjective judgement or other nonstatistical method, and (2) Type A errors, for which magnitudes are obtained statistically from a series of measurements.

All the Type B error components are assumed to be independent and to have rectangular or uniform distributions (that is, each has an equal probability of being within the region, $\pm\delta_i$, and zero probability of being outside that region. If the distribution is rectangular, the standard deviation, σ_s, for each Type B error component is equal to $\delta_i/3^{1/2}$ and the total "standard deviation" is $(\Sigma\sigma_s^2)^{1/2}$ where the summation is performed over all Type B error components.

The Type A errors are assumed to be independent, and the standard deviation, S_r, for each component is

$$S_r = \sqrt{\frac{\Sigma x^2 - \frac{(\Sigma x)^2}{N_r}}{N_r - 1}}, \qquad (11)$$

where the x values represent the individual measurements and N_r is the number of x values used for a particular Type A error component. The standard deviation of the mean is $S_r/N_r^{1/2}$, and the total standard deviation of the mean is $[\Sigma(S_r^2/N_r)]^{1/2}$, where the summation is carried out for all the Type A error components.

The expanded uncertainty is determined by combining the Type A and Type B "standard deviations" in quadrature and multiplying this result by an expansion factor of 2. The expanded uncertainty, U, is then

$$U = 2\sqrt{\Sigma\sigma_s^2 + \Sigma\frac{S_r^2}{N_r}}. \qquad (12)$$

When the monochromator-based measurement results are shifted to match the laser-based measurement results, there is an associated uncertainty added to the overall estimate. The value given with the calibration results, as a connector offset, is based on the residuals remaining after the monochromator-based data is shifted. The residuals are added in quadrature and the result is listed as a Type A uncertainty.

As illustrated in Table 3, the measurement uncertainty components are divided into two main categories and sometimes a third category is included depending on the customer request for calibration. The first category is devoted to the pyroelectric transfer standard calibration. The other category is devoted to the monochromator, light source, and other measurement equipment. In addition, there is uncertainty that is a consequence of properties inherent to the customer-provided meter.

6.1 Reference Detector

6.1.1 Calibration with Primary Standard (Type B)

Using measurement results obtained from calibrations with the NIST C-series calorimeter, the uncertainty of the absolute responsivity is 0.47 %. This measurement is available as a NIST Calibration Service and the uncertainty is well documented [2].

6.1.2 Temperature Stability (Type B)

Pyroelectric detectors have a strong temperature dependence (for lithium tantalate this is nearly 0.25 %/K) and therefore the reference detector, without active thermal stabilization, is the component in the measurement configuration most vulnerable to thermal drift. Therefore, the temperature of the reference detector is stabilized using a thermoelectric cooler in thermal contact with the insulated detector. The duration of the measurement for each wavelength increment is less than ten minutes. To estimate the uncertainty due to thermal drift, we have measured the temperature dependence of the reference detector for thirty minutes and calculated the responsivity drift to be 0.1 %. For a ten minute responsivity measurement at a given wavelength increment, we assign an uncertainty of 0.03 %.

6.1.3 Spatial Uniformity (Type A, n = 16)

The beam position for the duration of a calibration is highly repeatable. However, the PWTD was calibrated against the primary standard, using collimated laser sources with varying beam sizes, and was aligned manually several times for each wavelength. Therefore, we must account for variation of responsivity as a function of beam position when using the PWTD as a reference detector. This uncertainty contribution is an important consideration, given that one of the first assumptions made in deriving the measurement equation was that both the test and reference detectors have uniform spatial responsivity.

We measured the spatial uniformity (as stated in section 4.3) over the PWTD aperture area by use of a 0.3 mm diameter, circularly polarized, 674 nm laser beam as a probe. This probe beam was scanned across the aperture area at 0.1 mm intervals, while detector output data were collected. A total of 6400 data points were collected over an 8 mm × 8 mm area. The measurement results indicate that the maximum variation in detector response over an area approximately 5 mm in diameter, is less than 1 %. A subset of these data, 46 data points spaced 0.1 mm apart and 4.5 mm across the center of the detector, was analyzed and the standard deviation was 0.3 %; this value is used in our uncertainty estimate.

6.1.4 Linearity (Type B)

The radiant power throughput of the measurement system varies with wavelength. It is possible, by means of external feedback control, to adjust the throughput to a constant radiance. However, because of the concern for thermal stability and the need to minimize the measurement duration, we choose not to actively maintain constant radiance. Therefore, we must know the reference-detector linearity.

The radiant power output from the monochromator varies by nearly a factor of four as a function of wavelength, over the wavelength range, for both the 600 nm and 1000 nm blaze gratings. The typical worst-case range is approximately 25 μW to 100 μW. The linearity was evaluated at NIST, using a commercially available optical power meter [14]. The estimated value of this contribution was approximately 0.15 %.

6.1.5 Noise (Type A, n = 40)

During normal calibration at each wavelength, 40 samples are acquired from the reference detector and averaged. This is based on the standard deviation of the data $X(j)_{s1}$, $X(j)_{s2}$, $X(j)_{s3}$, ...$X(j)_{s40}$ described in Data Acquisition, section 5.5. Environmental factors, such as ambient acoustic noise (the reference detector, in addition to being pyroelectric is also piezoelectric), current amplifier noise, chopper instability, and other factors, contribute to white noise that appears as randomly varying output signal from the reference. Other noise, particularly 1/f noise, or drift is accounted for in the Temperature Stability component 6.1.2.

6.1.6 Repeatability (Type A, n = 3)

As stated in section 5.5, several samples from the test and standard reference detector are averaged at each wavelength increment. The result is three ratios, each having the form

$$\left(\frac{\frac{\sum_{i=1}^{5} X_{ti}}{5} - \frac{\sum_{i=1}^{5} b_{ti}}{5}}{\frac{\sum_{i=1}^{40} X_{si}}{40} - \frac{\sum_{i=1}^{40} b_{si}}{40}} \right)_{\lambda=j} \qquad (13)$$

This is repeated three times, once for each time the two-position mirror directs light to the test detector. These three ratios will vary from calibration episode to episode, but a typical worst-case value, based on the standard deviation of three 40-sample sets, over the 400 nm to 1800 nm wavelength range, is approximately 0.1 %.

6.2 Source Uncertainties

The source, the description of which was given in section 3, is optical radiation incident on the detector. Qualities of the source are affected by components such as the lamp, gratings, and mirror. The following facts should be considered in regard to source uncertainties.

- The wavelength is known, and the bandwidth is constant over the wavelength range of the measurement, with some tolerance, based on the physical construction of the monochromator.
- White noise and drift exist due to temperature change, current input variation, humidity change, and other factors.
- Electronic noise and acoustic noise affect the output of the reference detector, independent of wavelength.
- The lamp-filament image size is known and underfills the reference and test detectors.
- Gratings and mirrors polarize the lamp output.
- The test- and reference-detector electrical signal varies nearly linearly with optical input.

6.2.1 Monochromator Errors

6.2.1.1 Wavelength Offset (Type A, n = 3; Type B)

Worst-case uncertainty, based on wavelength calibration, can be measured by selecting a wavelength region in which detector responsivity is changing rapidly. For example, in the range from 1550 nm to 1560 nm, the absolute responsivity of a Ge photodiode varies by nearly 1 %/nm. A conservative estimate of the wavelength offset and mechanism backlash of the monochromator grating position is approximately 0.1 nm (using a HeNe laser at 1523 nm). Multiplying the detector responsivity rate of change by the wavelength offset yields a wavelength uncertainty of approximately 0.1 %.

6.2.1.2 Stray Light and Order Overlap (Type B)

The monochromator filters allow a certain amount of undesirable stray light and other-order transmission. When using a reference detector that is sensitive to a broad range of wavelengths, such as a pyroelectric detector, to measure the spectral responsivity of semiconductor-based photodetectors (and other thermal detectors), there is an uncertainty contribution that varies with wavelength and filter selection.

The amount of light transmitted by a glass filter is only *proportional* to the uncertainty contribution. For example, the short-wavelength cutoff filter may transmit as much as 0.1% stray light at 400 nm. But, the efficiency of other elements of the measurement system (for example, aluminum-mirror reflectance) may reduce this contribution further. Based on estimates of the grating efficiency and transmitivity, the contribution of uncertainty is approximately 0.5 % [9,10]. The data shown in Fig. 14 indicate this is a conservative estimate for most of the wavelength range for the measurement service.

The uncertainty at the shorter wavelength range of the monochromator is of special interest because of properties inherent to the Czerny-Turner monochromator configuration. When using the Czerny-Turner configuration, there is a measurable "out of band," re-entrant spectrum caused by reflection from the slit jaws and filter. The result of the reflection is unwanted stray light that is, over a broad spectrum, ranging *above* the filter cutoff (that is, longer wavelengths). This effect manifests itself as a low-power-level lamp spectrum propagated along the path of the desired monochromator output. The re-entrant spectra are significantly reduced to the level of the baseline-scattered light, by placement of a baffle at the focal point of the re-entrant spectra, within the monochromator. Two spectra are shown in Fig. 15; one curve (the lower curve) shows the residual background from 450 nm to 1000 nm, the other shows the output of a 674 nm wavelength laser diode. These two curves indicate that there is a small but measurable amount of background light, but there is no re-entrant spectrum at shorter wavelengths.

The filters are not calibrated in the strictest sense, rather they are evaluated to ensure that aging has not changed the cut-off wavelength or that the transmission *below* (i.e., shorter wavelengths) the cut-off has not increased. This evaluation is done by scanning a wavelength region of interest, using the reference detector, both with the filter in place and with the filter not in place. The ratio of these two scans will indicate the filter transmittance versus wavelength. At shorter wavelengths near 450 nm, this measurement becomes increasingly difficult. One reason for the difficulty is that the monochromator throughput is low and the signal for the condition of no-filter-in-place, as well as the condition of filter-in-place, is very near the noise floor of the reference detector. Therefore, the information from

the ratio of filter versus no-filter is limited by the low signal-to-noise ratio of the reference detector. Filters are selected to minimize stray light and the magnitude of light, reflected by the grating, that is any integer multiple of the wavelength of interest.

It is nearly impossible to quantify, experimentally or analytically, this uncertainty component. Therefore we rely on a conservative estimate (Type B, 0.29 %) that is based on our measured values from filter transmittance, as well as direct measurement of out-of-band transmission using laser sources at 633 nm, 674 nm, and 1523 nm.

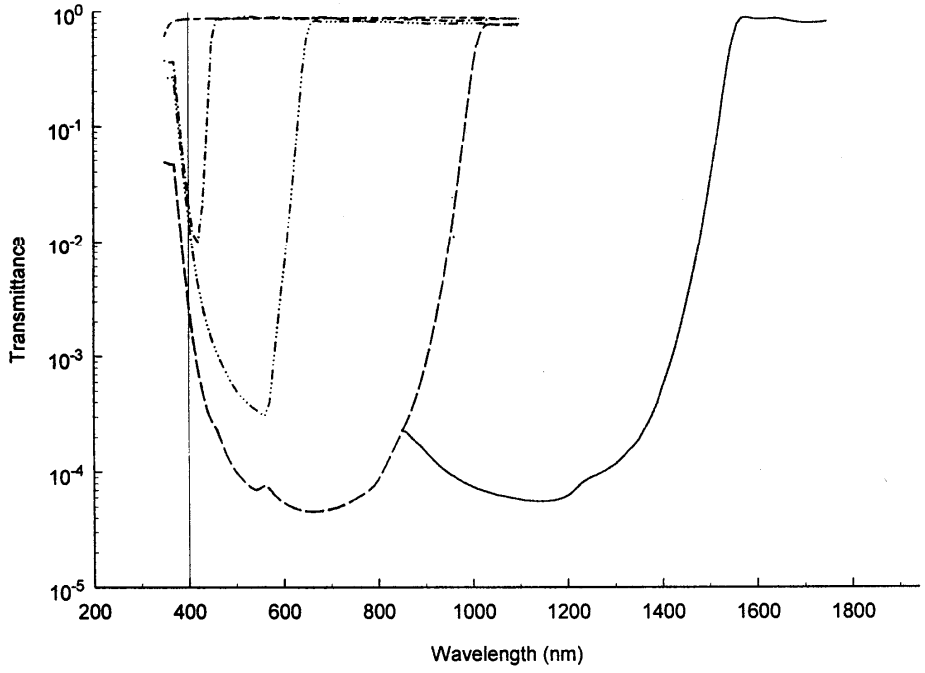

Figure 14. Measured, apparent (relative) glass-filter efficiency.

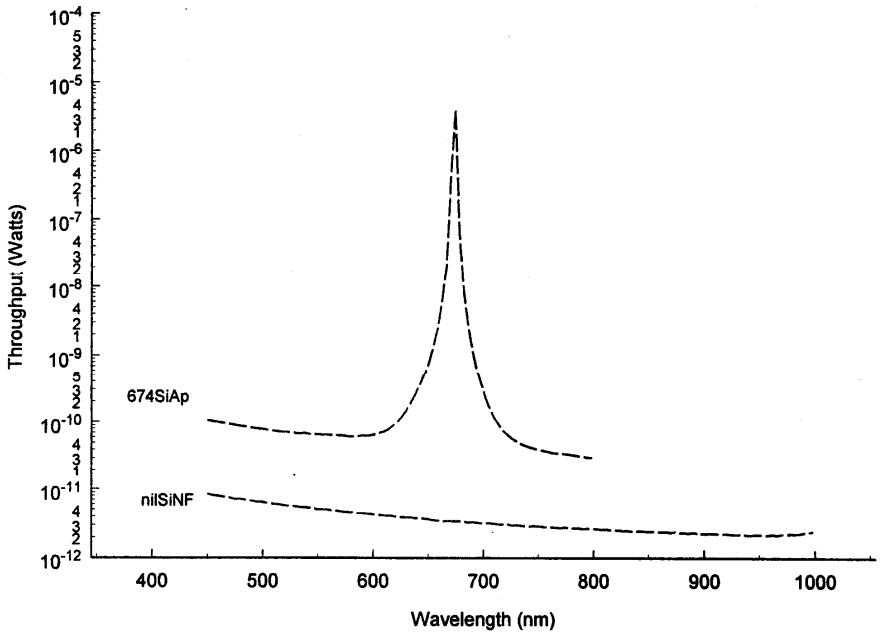

Figure 15. Monochromator throughput shown with 674 nm diode laser input and background.

6.2.1.3 Bandwidth Effect (Type B)

At any given monochromator-wavelength selection, the transmitted wavelength is actually a range $\Delta\lambda$ of wavelengths that is approximately 6 nm wide (that is, the bandwidth is not infinitely narrow under any circumstances). Therefore, when the monochromator is set at wavelength λ, there are photons, ranging in wavelength from λ to $(\lambda \pm \Delta\lambda/2)$, incident on the test detector. Photodiode sensitivity varies as a function of wavelength, and the amount of current generated by the photodiode is proportional to a weighted average of the photon energy within a band (the weighted average is a function of the slope of the detector responsivity over the selected band). Our transfer standard is a pyroelectric detector, which is a thermal detector and, therefore, does not exhibit the same behavior. However, a photodiode, even when calibrated against a thermal detector, may exhibit a change in responsivity over ±3 nm (6 nm) that may vary as much as 0.5 % [15].

6.2.2 Two-Position Mirror Reflectance (Type B)

Using reflectance data for a coated aluminum mirror at 900 nm, where the reflectance change is greatest, we have calculated an uncertainty contribution of 0.12 %. This uncertainty is based on the mirror reflectance being a function of the monochromator

output polarization. Both the reference detector and the test detector are situated relative to the final mirror (see hardware section), at an angle of approximately 22°. The estimate for the extent of misalignment (variation from 22°) is based on visual inspection of the beam position as a function of stage rotation, which has arcsecond resolution. The arcsecond resolution is well beyond what is perceivable. The uncertainty is based on the fact that, changing the rotary stage by 1° results in a beam realignment that is perceptible. In other words, 1° is within the resolution perceptible (a relative judgement) by the human operator.

6.2.3 Polarization (Type B)

The gratings used in the monochromator will slightly polarize the light from the broadband source. We have not measured the efficiency of the grating for two orthogonal, plane-polarization orientations; rather, we rely on the manufacturer's data [16]. The polarization uncertainty will depend on the polarization sensitivity of the detector under test, so we choose a worst-case scenario. Based on manufacturer's data for two orthogonal, plane-polarization orientations (normal and parallel to the grating surface) and on the worst-case polarization sensitivity of either gold-black-coated lithium tantalate, silicon, germanium, or indium gallium arsenide, the uncertainty contribution is less than approximately 0.01 %.

6.2.4 Beam Size (Type B)

Beam size depends on the imaging optics of the monochromator system and the filament dimensions. Using the mirror optics as described in earlier sections, the lamp filament is focused (1:1) on each detector. In addition, constant-intensity reduction of the beam size is accomplished by reducing the horizontal- and vertical-monochromator slit widths.

To verify the beam size, the beam image was measured at the focal plane (where the test or reference detector plane is located) using a scanning-slit, beam profilometer (average of 70 points for each slit-resolution increment). Data for the beam's spatial dimensions and relative intensity were stored in a file, and then the data were analyzed. Integrating the beam power over the scanning-slit, beam profilometer area indicates that 99.4 % of the beam is within a vertical dimension of 4 mm and 2 mm horizontal dimension. Therefore, less than 0.6 % of the beam is outside a rectangular beam image of 4 mm × 2 mm. If the test and reference detectors have identical detector areas, alignment depends on visual perception and the presence of the filament image on both the reference and test detector. Assuming that one can align the filament image on the detector active area, the question remains: what fraction of total input power does the perceived image represent? In other words, if properly aligned to intersect the center of the detector area, does the image fit within the detector area? The uncertainty is a function of the total optical power falling outside the detector area.

The reference detector aperture size is 5 mm in diameter. The size of test detectors measured by use of the system varies from customer to customer. For test detectors having an aperture size other than 5 mm, the uncertainty due to beam size may have to be evaluated on a case-by-case basis. For this document, a 0.3 % type B uncertainty is used as a conservative estimate; 0.6 % would be assigned if the test detector has an active area much larger (or smaller) than the reference.

6.3 Optical-Fiber Connector Correction (Type A, n = 3)

At each wavelength increment of the spectral scan, the output of the test detector is compared to the output of the NIST reference detector. This process is repeated a number of times for each detector and the results are averaged (this is discussed in section 5.5). As stated in the introduction, the test detector is also calibrated at several laser wavelengths using the NIST optical-fiber power measurement system (a single-mode optical fiber is connected to the test detector in these measurements). Example results from the monochromator-based system and the laser-based system, shown in table 2, are used together to obtain the results presented in table I of the Calibration Report. The residual offset values shown in column (4), are added in quadrature to obtain a single number and this number is considered a type A uncertainty, with n=3.

Table 2. Spectral responsivity measurement-offset residuals at three wavelengths (example data).

(1)	(2)	(3)	(4)
Wavelength (nm)	Monochromator-based absolute responsivity, shifted, interpolated (A/W)	Fiber connector-based absolute responsivity (A/W)	Residual offset [(2) – (3)]/(3) (%)
851.9	0.2199	0.2184	1.10
1310.0	0.7446	0.7352	1.28
1550.0	0.8294	0.8380	–1.03
quadrature sum, type-A uncertainty $(1.10^2 + 1.28^2 + (-1.03)^2)^{1/2}$			1.98

Table 3. NIST measurement uncertainties.

Source	Type B σ_s (%)	Type A S_r (%)	N_r
Pyroelectric working standard			
Calibration with Primary Standard	0.47		
Temperature stability	0.02		
Spatial uniformity		0.30	45
Linearity	0.09		
Repeatability		0.10	3
Noise		0.05	40
Spectral response measurements			
Wavelength calibration	0.06	0.10	3
Stray light	0.29		
Bandwidth (6 nm)	0.23		
Two-position mirror alignment	0.07		
Polarization	0.01		
Beam size	0.17		
Relative expanded uncertainty (k=2)	U =1.24 %		
Additional uncertainty due to optical-fiber connector correction (typical)		1.98	3
Relative expanded uncertainty (k=2)	U = 2.59 %		

7. Quality Control (Check-Standard Operation)

In addition to the reference-detector calibration and monochromator calibration, a check-standard operation is performed for each detector calibration or batch of calibrations. The operation follows the normal calibration procedure described in this document, over the wavelength range from 800 nm to 900 nm, at 10 nm increments. The check-standard operation is a quality control measure that verifies that the system performance results are comparable to previous results. Check-standard results are maintained in a separate record, one record for each customer.

The check standard is a six-element silicon photodiode trap detector, calibrated using the NIST laser optimized cryogenic radiometer (LOCR). The silicon-trap detector is based on photodiodes having nearly unit quantum efficiency (QE) over the wavelength range 800 nm to 900 nm. Therefore, in addition to historical records, the absolute spectral responsivity of the check standard can be quickly verified based on the LOCR calibration results, as well as mathematical calculation of the expected absolute responsivity. Though the wavelength range for the check-standard measurement is limited, it does overlap the wavelength range for each monochromator grating and represents a subset of coverage for any calibration request but requires less time than a complete, normal calibration routine.

We have tested several six-photodiode traps. One trap was built using 10 mm square, 300 μm thick silicon photodiodes and has been evaluated repeatedly. The absolute spectral current responsivity indicates that the optical-to-electrical energy conversion is quite high

and approaches the theoretically expected value for $\eta = 1$, where the absolute responsivity, i/P (current output/ optical input power) , is given by

$$\frac{i}{P} = \eta \frac{e}{h\nu} \cong \eta \frac{\lambda}{1239.5} \mathrm{AW^{-1}nm^{-1}} \tag{14}$$

for electron charge e, Planck's constant h, light frequency ν, and wavelength λ.

As an example, absolute spectral responsivity data for the 10 mm square embodiment are shown in Fig. 16 along with calculated values of $\lambda/1239.5$ (for light travelling in air). The results indicate that the measured responsivity value, measured at 10 nm increments, from 800 nm to 900 nm, is nearly 99 % of the theoretically expected value based on equation 14 (unit QE). The measurement results have an uncertainty of ±1.5 % (coverage factor k = 2), based on evaluation of the spectral responsivity measurement system using a NIST-calibrated reference detector.

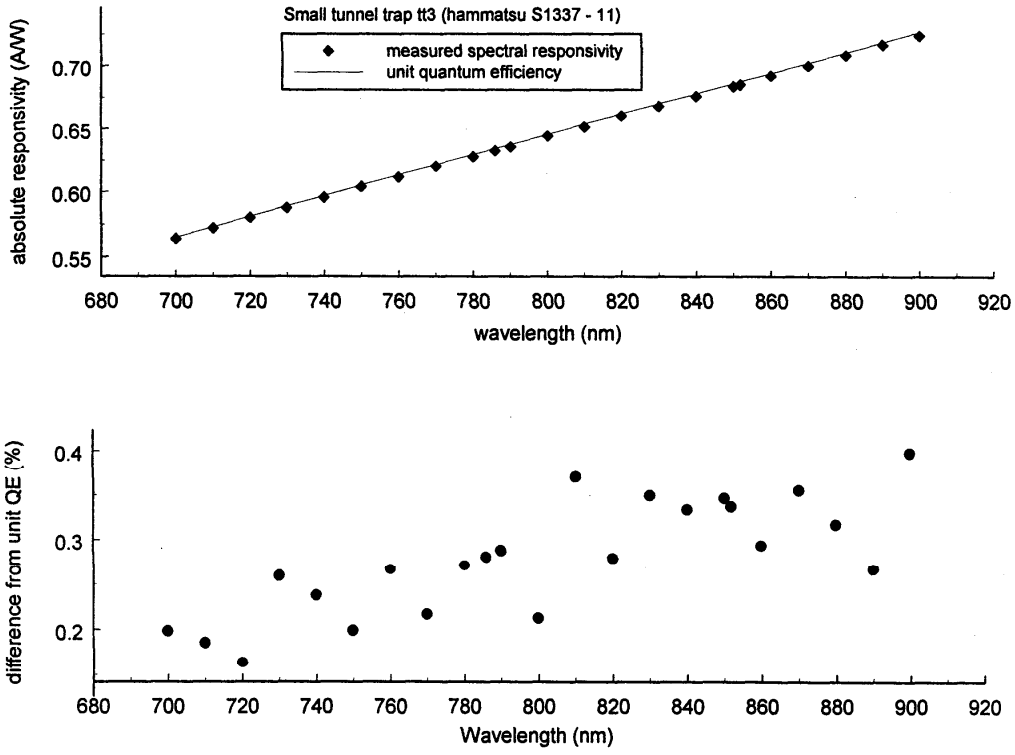

Figure 16. Absolute spectral responsivity of the check standard.

8. Conclusion

Absolute spectral responsivity calibration of laser and optical-fiber power meters over the wavelength range from 400 nm to 1800 nm presents many technical challenges. A single, continuously variable laser source is currently not available for this measurement, so we must rely on a broadband source and a monochromator, as well as several diode-laser sources for the power-meter input. The measurement uncertainty varies from customer to customer, depending on the power-meter detector configuration and the type of the fiber connector provided by the customer. We compare the laser and optical-fiber power meter response to a well characterized reference detector that is spatially and spectrally uniform and insensitive to varying input-beam coherence and geometry. The calibration service provides a written calibration record to the customer that includes a description of the measurement configuration, the absolute responsivity as a function of wavelength of the customer meter, and a documented estimate of the measurement uncertainty.

9. References

[1] Lehman, J.H.; Pyroelectric trap detector for spectral responsivity measurements. *Engineering and Laboratory Notes, Optics and Photonics News*, Vol. 8, No. 11, 1997, archived in *Appl. Opt.* Vol. 36, No. 34: pp. 9117-9118, 1997.

[2] West, E.D.; Case, W.E.; Rasmussen, A.L.; Schmidt, L.B.; A reference calorimeter for laser energy measurements. *Journal of Research of the National Bureau of Standards – A. Physics and Chemistry* 76A, No. 1: pp. 13-26; January-February 1972.

[3] Vayshenker, I.; Li, X.; Keenan, D.A.; Scott, T.R.; Errors due to connectors in optical fiber power measurements. *Symposium on Optical Fiber Measurements, Natl. Inst. Stand. Technol. Spec. Publ. 905*: pp. 49-52; 1996.

[4] Gallawa, R.L.; Li, X.; Calibration of optical fiber power meters: the effect of connectors. *Appl. Opt.* Vol. 26, No. 7: pp. 1170-1174; 1987.

[5] International Electrotechnical Comission (IEC); *Calibration of fibre optic power meters – CEI/IEC 1315.* Bureau Central de la Commission Electrotechnique Internationale, Geneva; 1995. (The standard includes formal definitions and background treatment of uncertainty contributions, including temperature dependence, nonlinearity, aging, beam geometry, connector effects, wavelength, bandwidth, and other considerations.)

[6] Lehman, J.; Sauvageau, J.; Vayshenker, I.; Cromer, C.; Foley, K.; Silicon wedge-trap detector for optical fibre power measurements. *Meas. Sci. Technol. 9*: pp. 1694-1698; 1998

[7] Harris, L.; The optical properties of metal blacks and carbon blacks. *Monograph Series No. 1:* Massachusetts Institute of Technology, Cambridge, Mass; p. 47, 1967.

[8] Kostkowski, H.J.; Nicodemus, F.E.; An Introduction to the Measurement Equation, Chapter 5, Self-Study Manual on Optical Radiation Measurements: Part I—Concepts, Chapters 4 and 5. *Nat. Bur. Stand. (U.S.), Tech. Note* 910-2; 1978.

[9] Strong, J.; *Concepts of Classical Optics, Appendix P*: W.H. Freeman & Company, San Francisco; 1958.

[10] James, J.F.; Sternberg, R.S.; *The Design of Optical Spectrometers*: Chapman and Hall, Ltd., London; p. 70; 1969.

[11] We use trade names to specify the experimental procedure adequately and do not imply or intend endorsement by the National Institute of Standards and Technology. Similar products by other manufacturers may work equally well.

[12] Day, G.W.; Hamilton, C.A.; Pyatt, K.W.; Spectral reference detector for the visible to 12-μm region; convenient, spectrally flat. *Appl. Opt.* Vol. 15, No.7: pp. 1865-1868; 1976.

[13] Taylor, B.N.; Kuyatt, C.E.; Guidelines for Evaluating and Expressing the Uncertainty of NIST Measurement Results. *Natl. Inst. Stand. Technol. Tech. Note 1297*: p. 8 1994.

[14] Vayshenker, I.; Yang, S.; Li, X.; Scott, T.R.; Nonlinearity of optical power meters. *Natl. Inst. Stand. Technol. Spec. Publ. 905*: pp. 101-104; 1996.

[15] Dereniak, E.L.; Crowe, D.G.; *Optical radiation detectors*: John Wiley and Sons, Inc., New York; pp. 105, 1984.

[16] McPherson Instrument, 7A Stewart Rd., Chelmsford, MA 01824.

Appendix A. Parts List

We use trade names to specify the experimental procedure adequately and do not imply endorsement by the National Institute of Standards and Technology. Similar products by other manufacturers may work equally well.

Monochromator, McPherson Model 207 with stepper motor and optical encoder
Grating, McPherson 140 mm × 140 mm, 600 lines/mm, 500 nm blaze
Grating, McPherson 140 mm × 140 mm, 600 lines/mm, 1000 nm blaze
Filter, 450 nm – 670 nm: OptoSigma 079-3340
Filter, 670 nm – 1075 nm: Schott LL 0650
Filter, 1075 nm – 1575 nm: Schott LL 1000
Filter, 1575 nm – 1800 nm: Schott RL 1500
Linear Positioning Stage, Newport PM500
Rotary Positioning Stage, Newport PM500
Optical Bench, Melles Griot
Lamp, Gilway Tungsten
Lamp Power Supply, HP
Lamp Hardware Mount, NIST
Lockin Amplifier, Stanford Research SR850
Current Amplifier, Stanford Research SR570
GPIB card, CEC
Software, CEC Testpoint
Pyroelectric Detector, NIST
Temperature Controller Electronics, ILX Lightwave
Temperature Controller Hardware Mount, NIST
Flat Mirror Mount, NIST
Flat Mirror, Front Surface Silver, New Focus
Gimbal Mirror Mount, NIST
Spherical Mirror, f/2 Front Surface Silver, Rocky Mountain Instrument
Light Tight box, NIST
Magnetic Component Base, Thorlabs

A.1 Mechanical Fixtures

Light Source Mount: The electrical connection of the bulb is attached to a ceramic bracket. The ceramic bracket is rigidly attached to a steel post that is attached to a magnetic base. The bulb is not enclosed or actively cooled.

Flat-Mirror Mounts: The flat mirrors are 50.8 mm in diameter and are epoxied to an aluminum L-shaped bracket mounted on a steel post. The steel post is mounted on a magnetic base and rests on the optical bench. The mirror is mounted such that it will rotate about the long axis of the steel post and the front surface of the mirror.

Spherical-Mirror Mounts: The f/2 spherical mirrors are mounted on gimbal mounts that rotate about the center axes of a 50.8 mm diameter spherical mirror. The mirror is held within an aluminum ring that is attached to a steel post. The steel post is mounted on a magnetic base and rests on the optical bench.

The f/4.7 spherical mirrors are mounted inside the monochromator. The mirror mounts are made of steel and are L-shaped. The mirrors rest on kinematic mounts that are aligned by the monochromator manufacturer. These mirrors are normally not re-adjusted.

Rotary Position Stage: The rotary stage supports one flat mirror on the output side of the monochromator. This stage supports the final mirror, which directs light alternately on each detector in the measurement setup. The manufacturer specification for the accuracy of the rotary stage is 0.1 μradian. Alignment of this mirror is critical to the accuracy of the overall measurement, because light from the grating monochromator is polarized and the mirror orientation is the only variable that changes between detectors for a given wavelength. The accuracy of this alignment is discussed in the error analysis section.

The combination of the rotary stage and mirror is used for several reasons. The primary reason is to accommodate the myriad commercial designs for optical-fiber power meters. The size of the meter and associated instrumentation requires a variety of working distances in proximity to the monochromator and reference detector. The two-position mirror arrangement allows room for cumbersome alignments. During operation, the time of stage travel from one measurement position to the other (from test position to reference position) must be minimized to shorten the duration of the calibration over the entire wavelength range of interest. The rotary stage, because of a small amount of necessary travel, is ideal for this application.

Grating Fixture: The grating fixture is a proprietary design patented by the manufacturer. The grating rests in a steel frame with three points of contact consisting of a ground-steel ball and two ground-steel cylinders that are embedded in the grating blank.

U.S. Department of Commerce
National Institute of Standards
and Technology
325 Broadway
Boulder, Colorado 80303-3328